



## Facile synthesis of PVA/CNTs for enhanced adsorption of $Pb^{2+}$ and $Cu^{2+}$ in single and binary system

Lingyun Jing<sup>a,b</sup>, Xiaoli Li<sup>a,\*</sup>

<sup>a</sup>College of Resources and Environmental Science, Lanzhou University, Lanzhou 730000, P.R. China, Tel. +86 931 8912438; Fax: +86 931 8912458; email: [lxli@lzu.edu.cn](mailto:lxli@lzu.edu.cn) (X. Li)

<sup>b</sup>College of Environmental and Municipal Engineering, Lanzhou Jiaotong University, West of Anning Road 88, Lanzhou 730070, P.R. China

Received 22 March 2015; Accepted 18 October 2015

### ABSTRACT

Multiwall carbon nanotubes (CNTs) were entrapped into polymer matrix by poly(vinyl alcohol) (PVA)-boric acid crosslinking. Thus, a novel macroporous composite adsorbent (PVA/CNTs) was obtained and used to remove heavy metal ions. Compared with CNTs, PVA/CNTs could effectively adsorb  $Pb^{2+}$  and  $Cu^{2+}$  from binary ion systems in the existence of HA,  $Zn^{2+}$ ,  $Cd^{2+}$ ,  $Ca^{2+}$ , and surfactant, respectively. The results indicated that sorption of  $Pb^{2+}$  and  $Cu^{2+}$  on PVA/CNTs was strongly dependent on pH values, and independent of ionic strength. PVA/CNTs beads exhibited special selectivity for  $Pb^{2+}$  ions in the presence of NaCl, anionic surfactant, and coexisting ions. The kinetic sorption can be described using a pseudo-second-order model very well. Chemical reaction such as surface complexation was the main sorption mechanism. The results from the sequential adsorption–desorption cycles showed that PVA/CNTs beads exhibited good desorption and reusability. The PVA/CNTs beads were prepared by a simple way and they are easily recovered from aqueous solution and efficiently regenerated. PVA/CNTs could be a promising alternative to activated carbon for wastewater treatment.

*Keywords:* PVA/CNTs; Selectivity; Anionic surfactant; Desorption

### 1. Introduction

The presence of heavy metal ions in various water resources has gained considerable attention.  $Pb^{2+}$  ion, one of the priority pollutants, may cause brain, bone, liver, and kidney damage and dysfunction of the central nervous system in human beings due to its cumulative effect [1,2]. Although  $Cu^{2+}$  ion is known to be an essential trace element to humans, higher  $Cu^{2+}$  intake can cause adverse effects. The maximum

acceptable concentration of  $Pb^{2+}$  and  $Cu^{2+}$  recommended by the World Health Organization (WHO) for drinking water is less than 0.01 and 2 mg/L [3], respectively. Therefore, removal of these toxic heavy metal ions before discharging them into the receiving systems is essential from the standpoint of environmental protection and public health.

Adsorption is one of the most effective and economical methods for the removal of heavy metal ions from aqueous solutions. In recent years, different kinds of adsorbents including activated carbon [4], zeolite [5], montmorillonite [6], Fly ash [7], mango

\*Corresponding author.

peel waste [8], orange peel [9], tea waste [10], rice husk [11], activated alumina [12], chitosan [13], various resins [14–16], and microorganisms [17–20] have been used to remove heavy metal ions from aqueous solutions. Activated carbon is an effective adsorbent for heavy metal ions removal. However, difficult separation from reaction solution, high regeneration cost, and mass loss limit its application in practical field. Therefore, there is a need to develop cost-effective, reusable, and energy-saving adsorbents for the removal of heavy metal ions from aqueous environment.

Poly(vinyl alcohol) (PVA) is a water-soluble material containing large amounts of hydroxyl groups. PVA has been widely applied in biomedical and pharmaceutical fields due to its low cost, non-toxicity, biocompatibility, good mechanical strength, and chemical stability. In our previous study, a new, economical, and eco-friendly way to prepare macroporous PVA beads has been developed in our lab to immobilize microorganism for wastewater treatment [21]. However, the resulting PVA beads showed low adsorption for heavy metal ions. Recently, the carbon nanotubes (CNTs) have been used as a promising adsorbent for the removal of various pollutants such as organic pollutants [22–25], dyes [26,27], and heavy metals [28–30] due to its large specific surface area, hollow and layered structures. However, CNTs with the nanosized structure have some disadvantages such as difficulty in separation of CNTs from the reaction system, mass loss and second pollution, which make it difficult to use in the batch and continuous systems.

In this work, we prepared a macroporous spherical composite of PVA and CNTs holding the advantages of both. The adsorption potential of PVA/CNTs beads as a new adsorption material to remove  $\text{Pb}^{2+}$  and  $\text{Cu}^{2+}$  from aqueous solution was investigated in detail. The adsorption process was studied in batch mode with regard to the effects of solution pH, initial metal ions concentration, contact time, salts, surfactant, and co-ions. To quantify and predict the adsorption behaviors of  $\text{Pb}^{2+}$  and  $\text{Cu}^{2+}$ , the ability of a number of existing isotherms and kinetic models were evaluated. Finally, the desorption efficiency and reusability of the adsorbents were assessed based on six consecutive adsorption–desorption cycles.

## 2. Experimental

### 2.1. Materials

Poly (vinyl alcohol) (PVA) with a degree of polymerization of 1,750 and an alcoholysis degree higher than 99% was obtained from Lanzhou Vinylon Factory

(Gansu, China). Multi-walled carbon nanotubes (CNTs) with outer diameter of 10–20 nm, length of 10–30  $\mu\text{m}$ , special surface area of about 200  $\text{m}^2/\text{g}$ , and –OH content of 3.06% were purchased from Chengdu Organic Chemicals Co. Ltd (Sichuan, China). Sodium dodecylsulphate (SDS), cetyltrimethylammonium bromide (CTAB), and all other chemicals were of analytical reagent grade. Distilled water was used to prepare all the solutions.

### 2.2. Preparation of macroporous PVA/CNTs beads

The synthetic scheme was shown in Fig. 1. In a typical synthesis, 6 g of PVA, 1.3 g of sodium alginate, and 7.5 g of  $\text{CaCO}_3$  were dispersed in 80 mL of distilled water and the solution was kept stirring in a boiling water bath for 2 h. One gram of CNTs was added into 20 mL of CTAB (0.5%) with an ultrasonic dispersion for 5 min. Then CNTs/CTAB mixture was added into the PVA/ $\text{CaCO}_3$  dispersion and the obtained dispersion was shaken at 90°C for 6 h. The product was extruded into a gently stirred 3%  $\text{CaCl}_2$ —saturated boric acid solution using a syringe. The stable crosslinked composite beads with diameter of approximately 3 mm formed and were immersed in the 3%  $\text{CaCl}_2$ —saturated boric acid solution for 48 h. At last, 1 mol/L of HCl was added into the solution to form porous beads. The macroporous beads were washed with distilled water to remove residual reagents.

### 2.3. Characterization of PVA/CNTs beads

The FT-IR spectra of PVA/CNTs before and after adsorption of  $\text{Pb}^{2+}$  and  $\text{Cu}^{2+}$  were obtained in the range of 4,000–500  $\text{cm}^{-1}$  using KBr pellets (NEXUS 670, Nicolet, USA). The thermal stability was studied with a Mettler Toledo Star thermogravimetric analyzer. X-ray diffraction (XRD) patterns of PVA and PVA/CNTs were recorded with a D/Max-2400 instrument (Rigaku, Japan) using Cu  $K\alpha$  radiation at 40 kV and 40 mA over the range ( $2\theta$ ) of 5°–70°. The surface morphology and microstructure of PVA/CNTs beads were also observed by means of a scanning electron microscope (SEM, HITACHI S-4800). The surface area, total pore volume, and average pore diameter of PVA/CNTs beads were determined by a Quantachrome NovaWin2 Instrument (USA). The concentration of  $\text{Pb}^{2+}$  and  $\text{Cu}^{2+}$  in the contact solution was determined with an inductively coupled plasma spectrometer (ICP/IRIS Advantage, Thermo).

Water content,  $W\%$ , represents the percentage of water held intrinsically by the beads. To estimate the

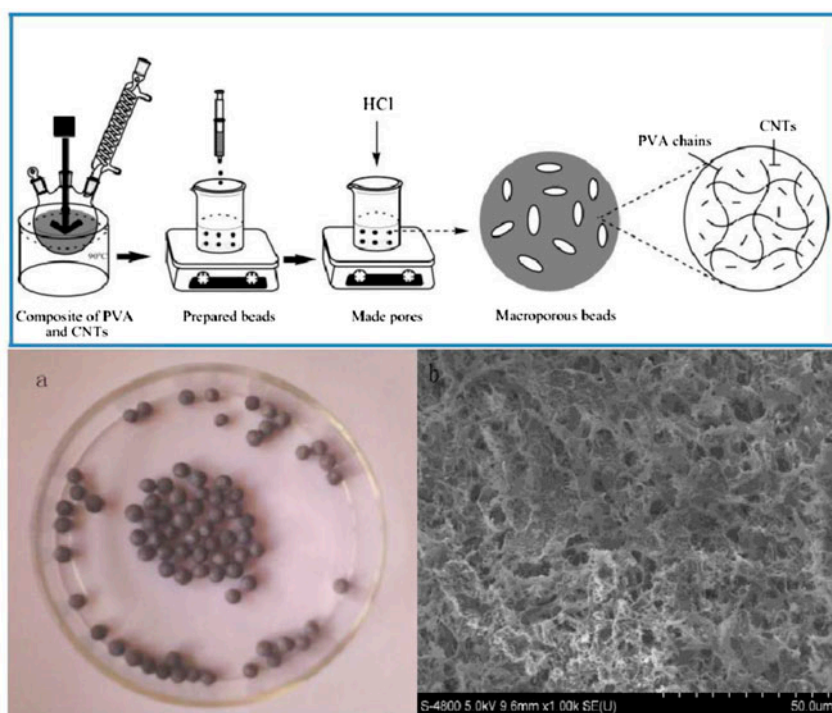


Fig. 1. Schema of synthetic route of macroporous PVA/CNTs beads and Surface morphologies of PVA/CNTs beads (a) digital photo and (b) microscopic image by SEM).

bulk density (BD) of dried PVA/CNTs beads, the frozen dried samples were filled in a 10 ml flask ( $W_1$ ) and were weighed ( $W_2$ ). The true density (TD) was measured as follows: a weighed amount of dried PVA/CNTs beads ( $W_0$ ) was placed into a 10 ml flask of known weight at 30°C. Into the flask was added 8 ml of cyclohexane and the mixture was kept at 30°C for 24 h. The flask was then filled with cyclohexane to the mark and was weighed ( $W$ ).  $W\%$ , BD and TD of PVA/CNTs beads are calculated using the following equations:

$$W\% = \frac{W_w - W_d}{W_w} \times 100 \quad (1)$$

$$BD = \frac{W_2 - W_1}{10} \quad (2)$$

$$TD = \frac{W_0}{10 - \frac{W - W_0}{d_c}} \quad (3)$$

where  $W_w$  and  $W_d$  are weights (g) of the wet and dried PVA/CNTs beads, respectively.  $W_2$  is the total weight of PVA/CNTs beads and the flask, and  $W_1$  is the weight of the flask only.  $W$  is the total weight of PVA/CNTs beads and the solvent.  $W_0$  is the weight of

the dry PVA/CNTs beads and  $d_c$  is the density of solvent ( $d_{\text{cyclohexane}} = 0.778$  g/ml).

#### 2.4. Adsorption experiments

Series batch tests for adsorption performances toward  $\text{Pb}^{2+}$  and  $\text{Cu}^{2+}$  onto PVA/CNTs were conducted using the bottle points methods. Stock solutions (1,000 mg/L) of  $\text{Pb}^{2+}$  and  $\text{Cu}^{2+}$  were prepared by dissolving appropriate amounts of  $\text{Pb}(\text{NO}_3)_2$  and  $\text{Cu}(\text{NO}_3)_2$ , respectively, in distilled water. Working solutions were prepared by diluting in distilled water. 0.5 M of HCl and NaOH were used to adjust the solution pH. The effect of pH on the adsorption of PVA/CNTs beads for  $\text{Pb}^{2+}$  and  $\text{Cu}^{2+}$  was evaluated in the pH range of 2.0–7.0. Adsorption equilibrium studies were carried out by contacting 0.1 g of PVA/CNTs beads with 50 mL of metal ions solution of different initial concentrations (50–500 mg/L) at pH of 6.0. In kinetic studies, 0.2 g adsorbents were added into 100 mL of  $\text{Pb}^{2+}$  ( $\text{Cu}^{2+}$ ) solution (50 mg/L) at pH of 6.0. Samples were taken at predetermined time intervals for the analysis of residual metal concentration in the aqueous solution. In order to determine the effect of salts and surfactant on  $\text{Pb}^{2+}$  and  $\text{Cu}^{2+}$  adsorption, the content of NaCl,  $\text{CaCl}_2$ , and SDS varied from 50 to

500 mg/L. The effect of co-existing ions on  $\text{Pb}^{2+}$  and  $\text{Cu}^{2+}$  adsorption was studied in the binary system of  $\text{Pb}^{2+}/\text{Zn}^{2+}$ ,  $\text{Pb}^{2+}/\text{Cu}^{2+}$ ,  $\text{Pb}^{2+}/\text{Cd}^{2+}$ ,  $\text{Cu}^{2+}/\text{Cd}^{2+}$ , and  $\text{Cu}^{2+}/\text{Zn}^{2+}$ , respectively, with the initial concentration of 50 mg/L for each metal ion. Furthermore, desorption experiments were investigated in batch mode.  $\text{Pb}^{2+}$  and  $\text{Cu}^{2+}$  loaded PVA/CNTs were regenerated with 0.1 M HCl. The solid samples were separated and washed thoroughly with distilled water. The regenerated adsorbents were reused in the next cycle of adsorption experiments.

The adsorption capacity at equilibrium ( $Q_e$ , mg/g), and the percentage removal (Removal, %) can be calculated using the following equations:

$$Q_e = \frac{(C_0 - C_e)V}{m} \quad (4)$$

$$\text{Removal (\%)} = \frac{C_0 - C_e}{C_0} \times 100 \quad (5)$$

where  $C_0$  and  $C_e$  (mg/L) are the initial and equilibrium concentrations of metal ions in the solution, respectively.  $V$  (L) is the volume of the solution and  $m$  (g) is the mass of the adsorbents.

### 3. Results and discussion

#### 3.1. Characteristics of PVA/CNTs beads

Water content, BD, and TD for PVA/CNTs beads were 86.10%, 0.055, and 1.639 g/mL, respectively. High water content value indicated the hydrophilic properties of PVA/CNTs beads, which facilitated the adsorption of heavy metal ions.

FTIR spectra of PVA and PVA/CNTs beads were analyzed (Fig. 2(a)). FTIR spectrum of PVA beads

showed the bands around 3,425.6, 1,637.5, 1,438.5, and 1,093.2  $\text{cm}^{-1}$ , which were attributed to the stretching of  $-\text{OH}$ ,  $-\text{COO}^-$  (asymmetric),  $-\text{COO}^-$  (symmetric), and  $\text{C}-\text{OH}$ , respectively. After the introduction of CNTs, the peaks were observed at 1,085.9 and 1,036.5  $\text{cm}^{-1}$  which were assigned to the stretching vibration of  $-\text{OH}$  groups in PVA and CNTs. PVA/CNTs beads with a large number of hydroxyl groups would exhibit excellent adsorption ability for heavy metal ions.

The PVA/CNTs beads also exhibited improved thermal stability in comparison with PVA beads. The results of thermal gravimetric analysis of PVA and PVA/CNTs beads were shown in Fig. 2(b). For PVA/CNTs beads, the weight loss of about 6.6% within the temperature range of 20–100°C may be attributed to the loss of surface adsorbed water. No obvious weight loss can be observed in the temperature range of 100–226°C, indicating thermal stability of PVA/CNTs. When temperature was higher than 288°C, the weight loss decreased significantly, which may be attributed to the decomposition of PVA/CNTs.

The XRD patterns for PVA and PVA/CNTs beads were given in Fig. 3(a). The diffraction peak at around 21.4° was a typical peak of the crystalline PVA. Its intensity increased significantly in composite of PVA/CNTs indicating that the crystalline structure of PVA enhanced after the introduction of CNTs. It may be due to the intermolecular and intramolecular hydrogen bonding between hydroxyl groups in both PVA and CNTs, resulting in the formation of a highly ordered network. Moreover, chemical crosslinking points were also established between the boric acid and hydroxyl groups in PVA [31]. As a result, the crystallinity degree, mechanical strength, and chemical stability were improved.

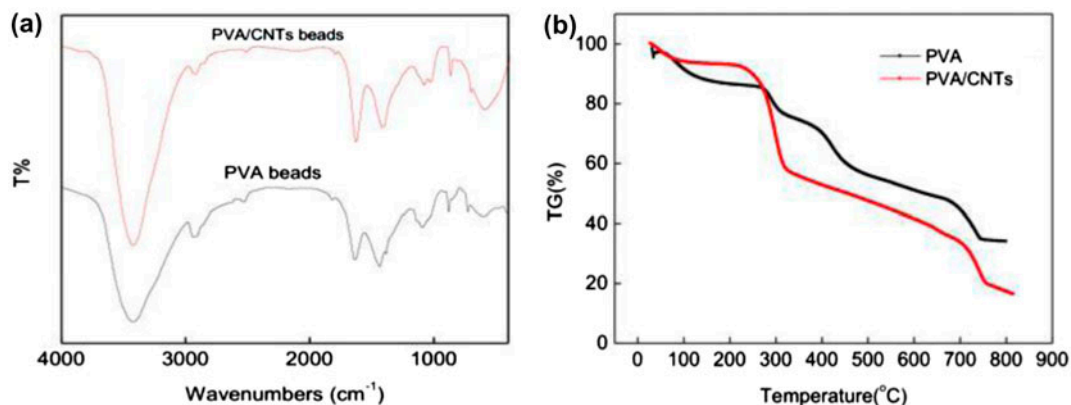


Fig. 2. FTIR spectra (a) and the thermogravimetry (TG) curves (b) of PVA and PVA/CNTs beads.

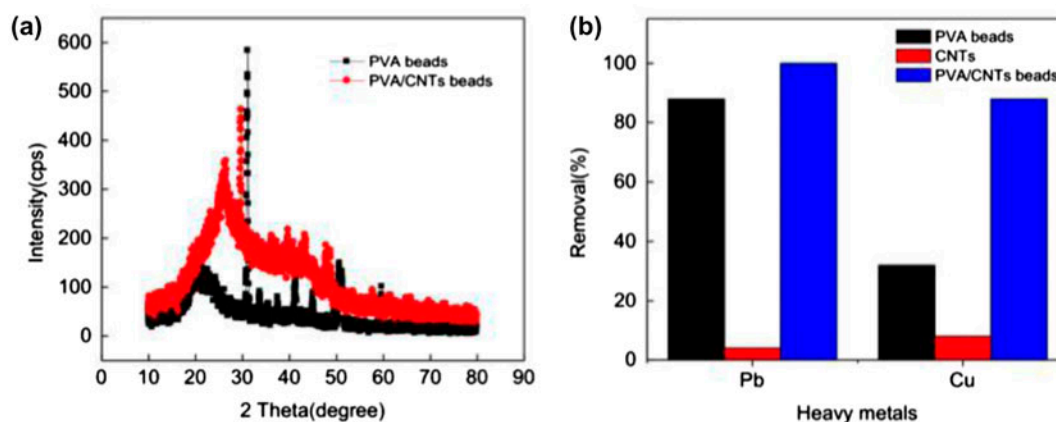


Fig. 3. XRD patterns of PVA and PVA/CNTs beads (a) and comparison of  $\text{Pb}^{2+}$  and  $\text{Cu}^{2+}$  ions adsorption on CNTs, PVA, and PVA/CNTs beads (b).

Fig. 1 showed the shape and surface morphologies of PVA/CNTs beads by digital camera and SEM. It can be seen from Fig. 1(a) that PVA/CNTs beads were perfectly spherical in shape with an average diameter of 3 mm and a rough surface. The surface area, total pore volume, and average pore diameter obtained for PVA/CNTs beads were  $29.17 \text{ m}^2/\text{g}$ ,  $0.0261 \text{ mL/g}$ , and  $26.93 \text{ nm}$ , respectively. As shown in Fig. 1(b), PVA/CNTs beads had many pores with different sizes. These pores could provide convenient diffusion channels for  $\text{Pb}^{2+}$  and  $\text{Cu}^{2+}$  ions into the inner of the beads. Higher surface area and porous structure are favorable for generating good adsorption capacity.

Fig. 3(b) showed the adsorption capacities of PVA/CNTs beads and PVA beads for  $\text{Pb}^{2+}$  and  $\text{Cu}^{2+}$  ions. It was obvious that the introduction of CNTs significantly improved the adsorption capacities for  $\text{Pb}^{2+}$  and  $\text{Cu}^{2+}$  ions. Hydroxyl groups in PVA and CNTs were the main active sites for heavy metal ions binding. In addition, the large surface area, porous structure, and special sites such as interstitial channels, grooves, and outside surface provided by multi-walled CNTs [32] would greatly benefit the adsorption of  $\text{Pb}^{2+}$  and  $\text{Cu}^{2+}$  ions.

### 3.2. Effect of initial solution pH

Fig. 4(a) showed the effect of solution pH on the adsorption of  $\text{Pb}^{2+}$  and  $\text{Cu}^{2+}$  by PVA/CNTs beads. It was found that the adsorption of  $\text{Pb}^{2+}$  and  $\text{Cu}^{2+}$  was highly dependent on pH mainly because pH affected the solubility of metal ions and changed the charge in the adsorbent surface. The percentage removal of  $\text{Pb}^{2+}$  increased from 61.39 to 100% with increase in pH from 2.0 to 5.0 and remained almost constant within

the range of pH 5.0–7.0. For  $\text{Cu}^{2+}$ , the percentage removal also increased with increase in pH from 1.0 to 6.0 and maximum adsorption of  $\text{Cu}^{2+}$  was observed at pH 6.0. With further increase in pH up to 7.0,  $\text{Cu}^{2+}$  ions precipitated as the insoluble hydroxides. Therefore,  $\text{Cu}^{2+}$  ions were removed by both adsorption and precipitation. At low pH, the competitive adsorption between protons and metal cations resulted in low adsorption of metal ions. Moreover, the protonation of the adsorbent surface did not favor the adsorption of positively charged metal cations due to the electrostatic repulsion. With increase in pH, the negative charge density on the adsorbent surface increased due to deprotonation of the metal binding sites and thus increased metal ions adsorption. Therefore, further adsorption experiments were carried out at optimum pH 6.0 for  $\text{Pb}^{2+}$  and  $\text{Cu}^{2+}$  ions.

### 3.3. Effect of initial metal concentration

The effect of initial metal concentration on the adsorption of PVA/CNTs beads for  $\text{Pb}^{2+}$  and  $\text{Cu}^{2+}$  ions was shown in Fig. 4(b). It was found that adsorption capacities of  $\text{Pb}^{2+}$  and  $\text{Cu}^{2+}$  ions on PVA/CNTs beads increased from 25.0 to  $196.3 \text{ mg/g}$  and 22.4 to  $130.5 \text{ mg/g}$ , respectively, as the initial metal ions concentration increased from 50 to  $500 \text{ mg/L}$  at 303 K. It was also observed that increasing initial metal concentration resulted in a decrease in the percent removal of metal ions. At an initial concentration of 50 and  $100 \text{ mg/L}$ , about 100% of  $\text{Pb}^{2+}$  and 89.7% of  $\text{Cu}^{2+}$  were removed using PVA/CNTs beads while 78.5% of  $\text{Pb}^{2+}$  and 52.2% of  $\text{Cu}^{2+}$  were removed at an initial concentration of  $500 \text{ mg/L}$ . It was evident that PVA/CNTs beads exhibited very strong affinity for  $\text{Pb}^{2+}$

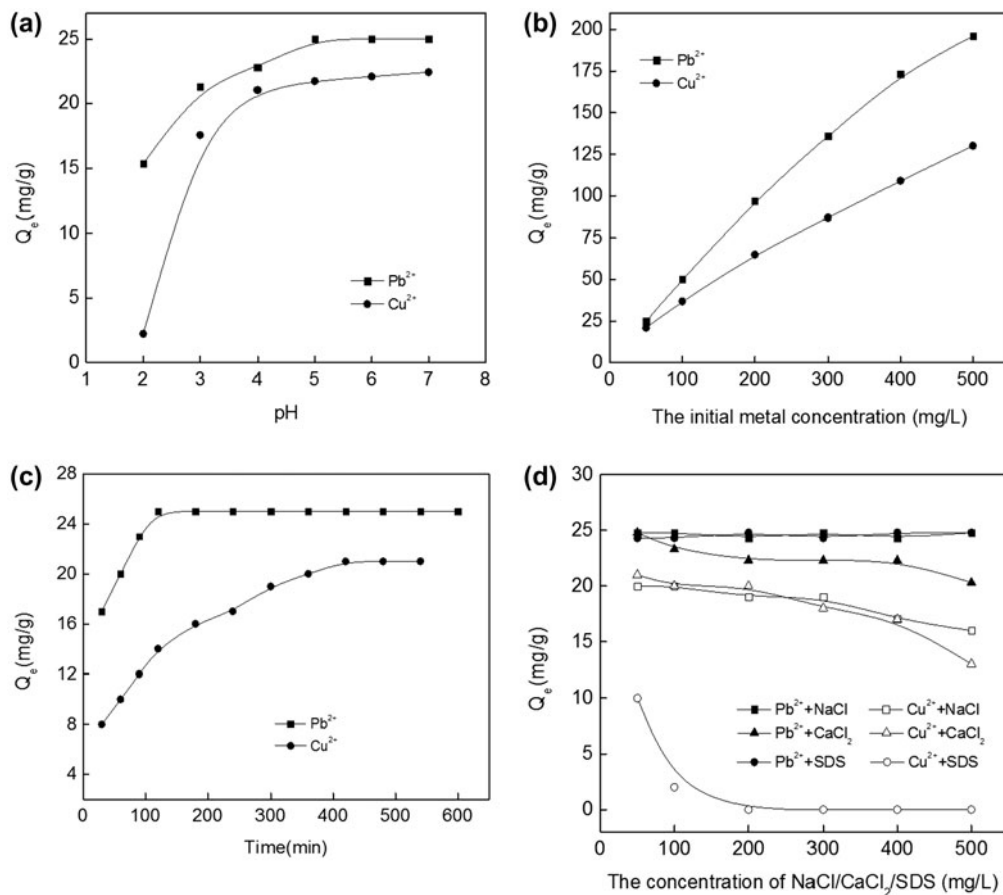


Fig. 4. Effect of pH (50 mL of solution with the initial concentration of 50 mg/L; PVA/CNTs: 0.1 g; 303 K) (a), the initial metal concentration (50 mL of solution with PVA/CNTs dosage of 0.1 g; pH 6.0; 303 K) (b), contact time (100 mL of solution with the initial concentration of 50 mg/L; PVA/CNTs: 0.2 g; pH 6.0; 303 K) (c), ionic strength and SDS (d) on the adsorption of  $Pb^{2+}$  and  $Cu^{2+}$  ions by PVA/CNTs beads (50 mL of solution with the initial concentration of 50 mg/L; PVA/CNTs: 0.1 g; pH 6.0; 303 K).

ions in comparison with  $Cu^{2+}$  ions, which may be due to the larger electronegativity and ionic radius of  $Pb^{2+}$  ions than  $Cu^{2+}$  ions.

### 3.4. Effect of contact time

The rate of metal ions adsorption is one of the important parameters for practical application of the adsorbents. The equilibrium adsorption of  $Pb^{2+}$  and  $Cu^{2+}$  ions on PVA/CNTs beads as a function of contact time was shown in Fig. 4(c). It can be seen that the amounts of  $Pb^{2+}$  and  $Cu^{2+}$  ions adsorbed increased with increase in contact time. The adsorption of  $Pb^{2+}$  ions on PVA/CNTs beads was very rapid and the equilibrium was reached at about 120 min. While the time required for copper solution to reach equilibrium was found to be 480 min. It was obvious that the adsorption rate of  $Pb^{2+}$  ions was significantly faster than that of  $Cu^{2+}$  ions. Hundred percent of  $Pb^{2+}$  ions

and 84% of  $Cu^{2+}$  ions were removed at equilibrium, respectively. Therefore, the contact time of 540 min was chosen as the optimum contact time for the adsorption of  $Pb^{2+}$  and  $Cu^{2+}$  ions onto PVA/CNTs beads.

### 3.5. Effect of salts in solution

The common cations such as  $Na^+$ ,  $K^+$ ,  $Ca^{2+}$ , and  $Mg^{2+}$  ions always coexist with heavy metal ions at a relatively high level in contaminated waters. The presence of salts may affect the adsorption behaviors of PVA/CNTs beads for heavy metal ions. This will require frequent regeneration and inevitably result in high operation cost in practice. Therefore, the effects of salts ( $NaCl$  and  $CaCl_2$ ) on the adsorption of  $Pb^{2+}$  and  $Cu^{2+}$  ions by PVA/CNTs beads were analyzed over the salt concentration range from 50 to 500 mg/L and the results were shown in Fig. 4(d). It was

obvious that increasing the concentration (50–500 mg/L) of NaCl in  $Pb^{2+}$  solutions had no effect on the adsorption of  $Pb^{2+}$  by PVA/CNTs beads. While a decrease of around 20% could be noted in  $Cu^{2+}$  adsorption as the concentration of NaCl in  $Cu^{2+}$  solutions increased from 50 to 500 mg/L. However,  $CaCl_2$  significantly decreased the adsorption of  $Pb^{2+}$  and  $Cu^{2+}$  ions under the similar experimental conditions, which maybe arise from the competitive effect between divalent metal ions and  $Ca^{2+}$  ions for the sites available. The adsorption efficiencies of  $Pb^{2+}$  and  $Cu^{2+}$  ions dramatically decreased by 18 and 38%, respectively, as the concentration of  $CaCl_2$  increased from 50 to 500 mg/L. According to Xu et al. [33], the potential in adsorption plane became less negative with increasing ionic strength, which decreased metal ions adsorption. The higher the valency of the index cation, the weaker the negative potential in the surface of adsorbent is. This may explain why  $CaCl_2$  had greater negative effect on the adsorption capacities of  $Pb^{2+}$  and  $Cu^{2+}$  ions than NaCl. In view of the above, PVA/CNTs beads

had the potential of removing  $Pb^{2+}$  and  $Cu^{2+}$  ions from wastewaters even in the presence of low concentrations of salts.

### 3.6. Effect of surfactant

Surfactants are usually present in real wastewaters at greater levels. They can interact with heavy metal ions by various reactions such as competitive binding, complexation, and/or electrostatic attraction. Therefore, it is very important to investigate the effect of surfactant on adsorption capacities of  $Pb^{2+}$  and  $Cu^{2+}$  ions by PVA/CNTs beads. As shown in Fig. 4(d), the adsorption of  $Pb^{2+}$  ions onto PVA/CNTs beads was not affected by the presence of the anionic surfactant (SDS), indicating that PVA/CNTs beads showed higher preference toward  $Pb^{2+}$  ions. However, the presence of SDS exhibited a significant negative effect on the adsorption of  $Cu^{2+}$  ions. The adsorption of  $Cu^{2+}$  ions was greatly depressed as the concentration of SDS in  $Cu^{2+}$  solution increased. This may be attributed to the formation of more stable complexes between  $Cu^{2+}$  ions and sulfonate groups. The higher selectivity of PVA/CNTs beads toward  $Pb^{2+}$  ions indicated that  $Pb^{2+}$  ions could be removed by using PVA/CNTs beads from the contaminated water containing SDS.

### 3.7. Competitive adsorption

The competitive adsorption was conducted in binary metal solutions ( $Cu^{2+}/Pb^{2+}$ ,  $Cu^{2+}/Zn^{2+}$ ,  $Cu^{2+}/$

$Cd^{2+}$ ,  $Pb^{2+}/Zn^{2+}$ , and  $Pb^{2+}/Cd^{2+}$ ). The initial concentration of each metal ion in the mixed solutions was 50 mg/L. The results were shown in Table 1. When PVA/CNTs beads were used to adsorb  $Pb^{2+}$  ions from  $Pb^{2+}/Cu^{2+}$ ,  $Pb^{2+}/Zn^{2+}$ , or  $Pb^{2+}/Cd^{2+}$  mixture, the removal efficiencies of  $Pb^{2+}$  ions were slightly influenced by the presence of  $Cu^{2+}$ ,  $Zn^{2+}$ , and  $Cd^{2+}$ . In binary system, the presence of  $Zn^{2+}$  ions had no obvious effect on the adsorption of  $Cu^{2+}$  ions by PVA/CNTs beads.  $Pb^{2+}$  ions, however, inhibited the adsorption of  $Cu^{2+}$  ions more seriously. The influence of co-existing ions on the adsorption of  $Cu^{2+}$  ions was in the following order:  $Pb^{2+} > Cd^{2+} > Zn^{2+}$ . It can be seen that the PVA/CNTs beads had high adsorption selectivity and high adsorption capacity for  $Pb^{2+}$  ions with the coexistence of  $Cu^{2+}$ ,  $Zn^{2+}$ , and  $Cd^{2+}$ . This can be applied to the separation or purification of  $Pb^{2+}$  ions in aqueous solutions containing  $Cu^{2+}$ ,  $Zn^{2+}$ , or  $Cd^{2+}$  ions.

### 3.8. Adsorption isotherms

In the present work, Langmuir, Freundlich, Tempkin, and Dubinin–Radushkevich (D–R) isotherms were used to describe the equilibrium between metal ions adsorbed onto the adsorbents and metal ions in the solution.

The Langmuir isotherm model assumes a monolayer adsorption on a homogenous surface where the binding sites have equal affinity and energy, and no interaction between the adsorbed species [34]. The linear form of the Langmuir isotherm model is given as:

$$\frac{C_e}{Q_e} = \frac{1}{K_L Q_{max}} + \frac{C_e}{Q_{max}} \quad (6)$$

where  $Q_e$  (mg/g) and  $C_e$  (mg/L) are the equilibrium metal concentrations in the solid and liquid phase,

Table 1  
Competitive adsorption in binary system (100 mL of solution with the initial concentration of each metal ion: 50 mg/L; PVA/CNTs: 0.2 g; 303 K; pH 6.0)

Metal system	Adsorption efficiency (%)			
	$Pb^{2+}$	$Cu^{2+}$	$Zn^{2+}$	$Cd^{2+}$
Single	100	89.72		
$Pb^{2+} + Cu^{2+}$	97.59	57.12		
$Pb^{2+} + Zn^{2+}$	99.53		75.34	
$Pb^{2+} + Cd^{2+}$	98.69			60.02
$Cu^{2+} + Zn^{2+}$		89.29	41.88	
$Cu^{2+} + Cd^{2+}$		80.15		5.46

respectively.  $Q_{\max}$  (mg/g) and  $K_L$  (L/mg) are the Langmuir constants related to saturated monolayer adsorption capacity and the binding energy of the sorption system, respectively.

The Freundlich isotherm assumes that the adsorption of metal occurs on a heterogeneous surface by multilayer adsorption and that the amount of adsorbate adsorbed increases infinitely with increase in concentration [35]. The linearized Freundlich isotherm model is expressed as:

$$\ln Q_e = \ln K_f + \frac{1}{n} \ln C_e \quad (7)$$

where  $K_f$  and  $n$  are the Freundlich constants, indicating the relative adsorption capacity and the adsorption intensity, respectively.

Tempkin isotherm is based on the assumption that the decline of the heat of adsorption as a function of temperature is linear rather than logarithmic [36]. The linearized Tempkin isotherm model is given as:

$$Q_e = B_T \ln A_T + B_T \ln C_e \quad (8)$$

where  $B_T = (RT)/b_T$ ,  $b_T$  is the Tempkin constant related to the heat of adsorption (kJ/mol).  $A_T$  is the equilibrium binding constant corresponding to the maximum binding energy (L/g).  $R$  is the gas constant (8.314 J/(mol K)), and  $T$  is the absolute temperature (K).

The D–R isotherm is more general than the Langmuir isotherm since it does not assume a homogeneous surface or constant sorption potential. It can be applied to distinguish between physical and chemical adsorption [37,38]. The linear form of D–R isotherm equation is expressed as:

$$\ln Q_e = \ln Q_m - \beta \varepsilon^2 \quad (9)$$

where  $\beta$  is a constant related to the mean free energy of adsorption ( $\text{mol}^2 \text{J}^{-2}$ ),  $Q_m$  is the theoretical saturation capacity (mg/g),  $\varepsilon$  is the Polanyi potential, which is equal to  $RT \ln(1 + 1/C_e)$ . The mean adsorption energy,  $E$  (kJ/mol), was involved in the transfer of free energy of one mole of metal ions from infinity in solution to the surface of the solid. The value of  $E$  can be determined by the following equation:

$$E = \frac{1}{(2\beta)^{1/2}} \quad (10)$$

where  $E$  value gives information about adsorption mechanism, physical or chemical. If the value of  $E$  is between 8 and 16 kJ/mol, the adsorption process takes

place chemically and if the value of  $E$  is less than 8 kJ/mol, then the adsorption process takes place physically [39].

The isotherm data of  $\text{Pb}^{2+}$  onto PVA/CNTs has been linearized using Langmuir, Freundlich, Tempkin, and Dubinin–Radushkevich (D–R) isotherm equations as shown in Fig. 5. The constants along with the correlation coefficients ( $R^2$ ) were listed in Table 2. As can be seen from Table 2, higher correlation coefficient ( $R^2 > 0.98$ ) was obtained from the Langmuir model, indicating that the Langmuir isotherm model correlated well with the equilibrium data for  $\text{Pb}^{2+}$  ions adsorption on PVA/CNTs beads. The theoretical  $Q_{\max}$  value (comparison with the reported values were shown in Table 3) was in good agreement with that obtained experimentally as seen in Table 2. While for  $\text{Cu}^{2+}$  ions, lower  $R^2$  value showed that the Langmuir model was not suitable for modeling the  $\text{Cu}^{2+}$  adsorption onto PVA/CNTs beads. The Freundlich isotherm model gave the highest  $R^2$  values larger than 0.98, indicating that the adsorption of  $\text{Pb}^{2+}$  and  $\text{Cu}^{2+}$  ions onto PVA/CNTs beads was best described by this isotherm. The values of  $n$  representing the favorability of the adsorption were more than one, indicating that the adsorption of  $\text{Pb}^{2+}$  and  $\text{Cu}^{2+}$  ions on PVA/CNTs beads was favorable at the studied conditions. The Freundlich isotherm model fitted the equilibrium data very well. This may be attributed to the heterogeneity of various active sites on the surface of PVA/CNTs beads. To evaluate the adsorption potential of PVA/CNTs beads for  $\text{Pb}^{2+}$  and  $\text{Cu}^{2+}$  ions, the Tempkin isotherm constants ( $A_T$  and  $b_T$ ) were calculated. The value of  $A_T$  obtained for  $\text{Pb}^{2+}$  ions was larger than that for  $\text{Cu}^{2+}$  ions which indicated a better potential for  $\text{Pb}^{2+}$  ions. As shown in Table 2, the D–R isotherm gave the lower correlation coefficients and the theoretical  $Q_m$  values and the experimental  $Q_{\text{exp}}$  values were not in agreement with each other indicating a poor D–R isotherm model fit.

### 3.9. Adsorption kinetics

In order to investigate the kinetic mechanism that controls the adsorption of  $\text{Pb}^{2+}$  and  $\text{Cu}^{2+}$  ions onto PVA/CNTs beads, the pseudo-first-order, the pseudo-second-order, and intraparticle diffusion models are used to analyze the equilibrium data.

The pseudo-first-order equation is given as:

$$\ln(Q_e - Q_t) = \ln Q_e - K_1 t \quad (11)$$

where  $Q_e$  (mg/g) and  $Q_t$  (mg/g) are the adsorption capacities at equilibrium and at time  $t$  (min), respectively.  $K_1$  is the first-order rate constant (1/min).

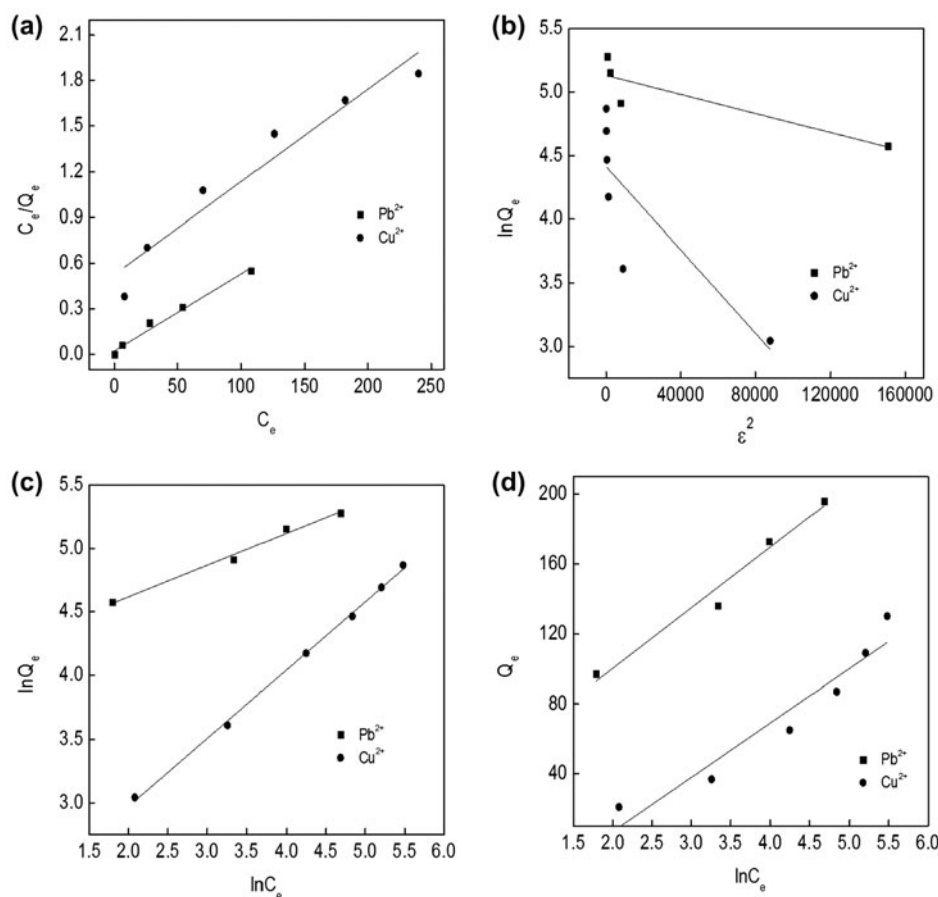


Fig. 5. Langmuir (a), Freundlich (b), Temkin (c), and Dubinin–Radushkevich (D–R) (d) isotherm for Pb<sup>2+</sup> and Cu<sup>2+</sup> ions adsorption by PVA/CNTs beads.

Table 2  
Adsorption isotherms for Pb<sup>2+</sup> and Cu<sup>2+</sup> ions adsorption onto PVA/CNTs beads (100 mL of solution; 0.2 g of PVA/CNTs: 303 K, pH of 6.0)

Isotherm constants		Pb <sup>2+</sup>	Cu <sup>2+</sup>
Langmuir	$Q_{exp}$ (mg/g)	196.3	130.5
	$Q_{max}$ (mg/g)	196.08	163.93
	$K_L$ (L/mg)	0.22	0.01
	$R^2$	0.9854	0.9395
Freundlich	$K_f$ (L/g)	61.52	6.71
	$n$	4.01	1.87
	$R^2$	0.9892	0.9985
Tempkin	$b_T$ (J/mol)	72.62	81.13
	$A_T$ (L/g)	2.43	0.17
	$R^2$	0.9740	0.9261
D–R isotherm	$Q_m$ (mg/g)	169.14	82.41
	$E$ (kJ/mol)	0.35	0.16
	$R^2$	0.7950	0.6813

The pseudo-second-order model developed by Srividya and Mohanty [39] assumes that the adsorption capacity of adsorbent is proportional to the number of active sites on its surface. The pseudo-second-order equation is expressed as:

$$\frac{t}{Q_t} = \frac{1}{K_2 Q_e^2} + \frac{t}{Q_e} \tag{12}$$

where  $K_2$  is the second-order rate constant (g/(mg min)). Additionally, the initial adsorption rate,  $h$  (mg/(g min)) can be determined from  $K_2$  and  $Q_e$  values using  $h = K_2 Q_e^2$ .

The intraparticle diffusion model assumes a two-step adsorption process-metal ions binding to the adsorbent surface followed by metal ions diffusion through its pores. Intraparticle diffusion equation is given as [40]:

$$Q_t = K_p t^{0.5} + C \tag{13}$$

Table 3  
Comparison of  $\text{Pb}^{2+}$  and  $\text{Cu}^{2+}$  adsorption on PVA/CNTs beads with other adsorbents

Adsorbents	$Q_e^a$ (mg/g)		Refs.
	$\text{Cu}^{2+}$	$\text{Pb}^{2+}$	
Natural zeolite	8.97	–	[41]
Active carbon	–	6.68	[42]
Fly ash	–	4.98	[42]
Activated alumina	–	83.33	[12]
Steel slag	16.21	32.26	[43]
Tartaric acid modified rice husk	29	108	[11]
Dithiocarbamated-sporopollenin	17.4	94.7	[44]
Non-living <i>Spirogyra neglecta</i>	115.3	116.1	[19]
<i>Caulerpa lentillifera</i>	42.38	28.72	[20]
Valonia tannin resin	45.44	138.9	[16]
$\text{HNO}_3$ oxidized CNTs	24.49	97.08	[28]
$\text{HNO}_3$ oxidized CNT sheets	64.93	117.65	[29]
CNTs/calcium alginate composites	–	78.74	[45]
$\text{MnO}_2$ -coated CNTs	84.88	–	[46]
PVA/Sclg cryogels	791.5	–	[47]
PVA/CNTs beads	130.5	196.3	Present work

<sup>a</sup>The Langmuir maximum capacity.

where  $K_p$  is the intraparticle diffusion constant ( $\text{mg}/(\text{g min}^{0.5})$ ) and  $C$  represents the boundary layer diffusion effect. If the linear plot of intraparticle diffusion passes through the origin, then the intraparticle diffusion is the only rate-limiting step. Otherwise, some other mechanism along with intraparticle diffusion is also involved.

Fig. 6 shows the linear plots of pseudo-first-order and second-order model for  $\text{Pb}^{2+}$  adsorption onto PVA/CNTs beads. The pseudo-first-order constants ( $Q_e$ ,  $K_1$  and  $R^2$ ) were presented in Table 4. The theoretical  $Q_e$  values did not agree with the experimental values, and the correlation coefficients were also found to be low. These results indicated that the pseudo-first-order kinetic model was not suitable for

modeling  $\text{Pb}^{2+}$  and  $\text{Cu}^{2+}$  ions adsorption onto PVA/CNTs beads. The application of the second-order kinetic model by plotting  $t/Q_t$  vs.  $t$  yielded the second-order rate constant ( $K_2$ ), estimated equilibrium capacity ( $Q_e$ ), and the regression coefficients ( $R^2$ ). As can be seen from Table 4, the calculated  $Q_e$  values showed a good agreement with the experimental values and the obtained values for coefficients of determination ( $R^2$ ) were more than 0.995, which indicated that the pseudo-second-order kinetic model described well the removal of  $\text{Pb}^{2+}$  and  $\text{Cu}^{2+}$  ions by PVA/CNTs beads as adsorbents. These results indicated that the rate-limiting step in the adsorption of  $\text{Pb}^{2+}$  and  $\text{Cu}^{2+}$  ions was chemisorption involving valence forces through the sharing or exchange of electrons between

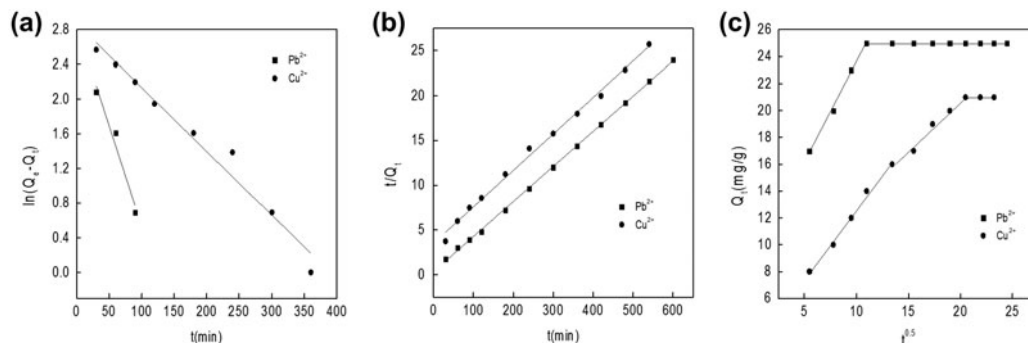


Fig. 6. The pseudo-first-order (a), pseudo-second-order (b), and intraparticle diffusion (c) plot for  $\text{Pb}^{2+}$  and  $\text{Cu}^{2+}$  ions adsorption onto PVA/CNTs beads.

Table 4

Kinetic parameters of pseudo-first order and pseudo-second order for Pb<sup>2+</sup> and Cu<sup>2+</sup> ions adsorption onto PVA/CNTs beads (100 mL solution of the initial concentration of each metal ion: 50 mg/L; PVA/CNTs: 0.2 g; 303 K)

Kinetics	Kinetic constants	Pb <sup>2+</sup>	Cu <sup>2+</sup>
Pseudo-first-order	Q <sub>exp</sub> (mg/g)	25.00	21.03
	Q <sub>e</sub> (mg/g)	17.24	17.60
	K <sub>1</sub> (× 10 <sup>-2</sup> ) (1/min)	2.31	0.74
	R <sup>2</sup>	0.9666	0.9728
Pseudo-second-order	Q <sub>e</sub> (mg/g)	25.51	24.57
	K <sub>2</sub> (× 10 <sup>-3</sup> ) (g/(mg min))	4.34	0.47
	h (mg/(g min))	2.83	0.28
	R <sup>2</sup>	0.9995	0.9953
Intraparticle diffusion	K <sub>p1</sub> (mg/(g min <sup>1/2</sup> ))	1.482	1.041
	R <sup>2</sup>	0.9972	0.9933
	K <sub>p2</sub> (mg/(g min <sup>1/2</sup> ))	–	0.785
	R <sup>2</sup>	–	0.9782

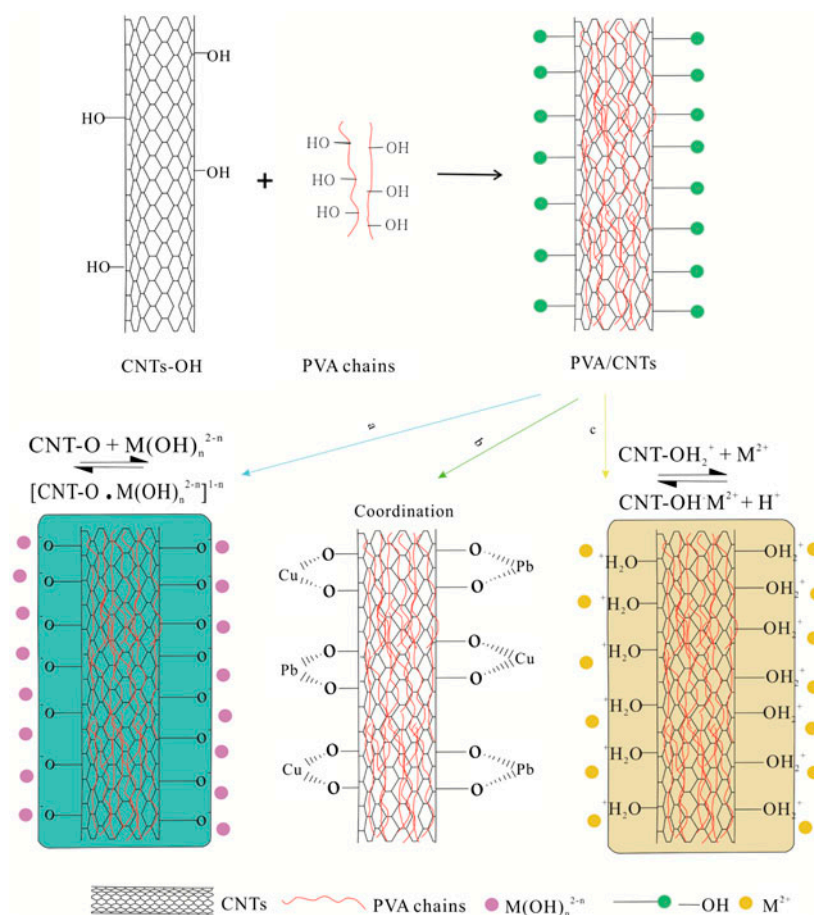


Fig. 7. The proposed mechanism of Pb<sup>2+</sup> and Cu<sup>2+</sup> ions adsorption onto PVA/CNTs beads.

adsorbent and metal ions. PVA/CNTs beads had a large number of hydroxyl groups, which can interact with metal ions through complexation, ion exchange, and/or electrostatic attraction. In addition, physical adsorption may be responsible for the interaction between PVA/CNTs beads and metal ions because PVA/CNTs beads had a large surface area and macroporous structure. The  $h$  and  $K_2$  values calculated from the pseudo-second-order kinetic model were higher for  $\text{Pb}^{2+}$  ions than for  $\text{Cu}^{2+}$  ions, indicating that the removal rate of  $\text{Pb}^{2+}$  ions by PVA/CNTs beads was much faster than that of  $\text{Cu}^{2+}$  ions. These results were consistent with the results obtained from the experimental process.

PVA/CNTs bead is a porous adsorbent, so the diffusion process may affect the adsorption process. Fig. 6(c) showed the intraparticle diffusion plots of  $\text{Pb}^{2+}$  and  $\text{Cu}^{2+}$  ions adsorption onto PVA/CNTs beads. It can be seen that  $\text{Pb}^{2+}$  and  $\text{Cu}^{2+}$  ions exhibited different diffusion kinetics. For  $\text{Pb}^{2+}$  ions, there was only one stage. While for  $\text{Cu}^{2+}$  ions, a three-stage adsorption occurred: the initial curved stage was attributed to rapid external diffusion and surface adsorption, the second stage was the gradual adsorption stage where intraparticle diffusion was the rate limiting step, and the third stage was the final equilibrium stage where intraparticle diffusion started to slow down due to extremely low metal concentration in the solution. The intraparticle diffusion parameter,  $K_p$  ( $\text{mg}/(\text{g min}^{-0.5})$ ), was calculated and shown in Table 4. The higher  $K_{p1}$  value for  $\text{Pb}^{2+}$  ions than for  $\text{Cu}^{2+}$  ions indicated that the faster adsorption of  $\text{Pb}^{2+}$  ions from the bulk phase to the exterior surface of PVA/CNTs beads, showing that PVA/CNTs beads exhibited stronger preference for  $\text{Pb}^{2+}$  ions than for

$\text{Cu}^{2+}$  ions. For  $\text{Cu}^{2+}$  ions, the  $K_{p1}$  value was much greater than the  $K_{p2}$  value, and the last rate constant was close to zero implying the attained equilibrium state. Based on the results it was suggested that both surface adsorption and intraparticle diffusion affected  $\text{Cu}^{2+}$  adsorption onto PVA/CNTs beads, while surface adsorption was the main mechanism for  $\text{Pb}^{2+}$  adsorption. Based on the above results, the adsorption mechanisms of  $\text{Pb}^{2+}$  and  $\text{Cu}^{2+}$  onto PVA/CNTs beads were proposed as shown in Fig. 7.

### 3.10. Desorption and reusability

In order to make the adsorption process more economical and feasible through repeated use of the adsorbents, desorption efficiency and regeneration potential of PVA/CNTs beads were studied. Desorption experiments were performed maintaining the process similar to the batch experiments. 0.1 M HCl was able to effectively elute the adsorbed metal ions from PVA/CNTs beads, 96 and 95% of the adsorbed  $\text{Pb}^{2+}$  and  $\text{Cu}^{2+}$  ions were desorbed, respectively. To test the reusability of PVA/CNTs beads, adsorption–desorption cycles were repeated six times by using the same adsorbents. Fig. 8 showed the adsorption capacities of PVA/CNTs beads for  $\text{Pb}^{2+}$  and  $\text{Cu}^{2+}$  ions over six successive adsorption–desorption cycles. The results indicated that the adsorption capacities of  $\text{Pb}^{2+}$  and  $\text{Cu}^{2+}$  ions slightly decreased with increase in adsorption–desorption cycle, at the end of the sixth cycle, more than 92 and 73% of  $\text{Pb}^{2+}$  and  $\text{Cu}^{2+}$  ions were removed by PVA/CNTs beads, respectively. The reusability of PVA/CNTs beads decreased the operation cost and indicated the industrial applicability. Therefore, PVA/CNTs beads were a good reusable adsorbent and could be successfully applied for the recovery of heavy metal ions from water and wastewater.

## 4. Conclusions

In this work, we prepared a macroporous poly (vinyl alcohol)/carbon nanotubes (PVA/CNTs) beads using a facile method. PVA/CNTs beads held advantages of both PVA and CNTs: easy separation and excellent adsorption ability for heavy metal ions. The resulting beads with porous structure exhibited good mass transfer property and high stability. The addition of CNTs increased the adsorption capacities of  $\text{Pb}^{2+}$  and  $\text{Cu}^{2+}$  ions significantly. The equilibrium data of  $\text{Pb}^{2+}$  and  $\text{Cu}^{2+}$  ions were best described by the Freundlich isotherm. The adsorption kinetics followed the pseudo-second-order kinetic model with rapid adsorption rate. Based on intraparticle diffusion model, it was found that the main mechanism for  $\text{Pb}^{2+}$  ions

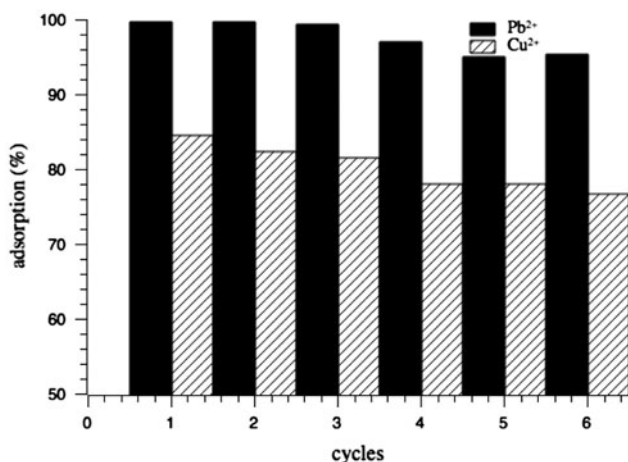


Fig. 8. Adsorption efficiencies of PVA/CNTs beads after repeated adsorption–desorption operations.

adsorption onto PVA/CNTs beads was surface adsorption, while  $\text{Cu}^{2+}$  ions adsorption may be controlled by surface adsorption at earlier stages and later by intraparticle diffusion.  $\text{CaCl}_2$  had greater negative effect on the adsorption capacities of  $\text{Pb}^{2+}$  and  $\text{Cu}^{2+}$  ions than  $\text{NaCl}$ . The presence of anionic surfactant (SDS) had no obvious effect on  $\text{Pb}^{2+}$  adsorption, but the adsorption of  $\text{Cu}^{2+}$  decreased significantly at the same conditions. The competitive adsorption showed that PVA/CNTs beads had a markedly high selectivity for  $\text{Pb}^{2+}$  with the coexistence of  $\text{Cu}^{2+}$ ,  $\text{Zn}^{2+}$ , and  $\text{Cd}^{2+}$ . Therefore, it could be concluded that PVA/CNTs beads were an eco-friendly, efficient, and reusable adsorbent for removal of heavy metals from aqueous solution.

### Acknowledgements

The authors gratefully acknowledge the financial supports from the National Natural Science Foundation of China (No. 21407071) and the Fundamental Research Funds for the Central Universities (lzujbky-2014-123).

### References

- [1] E. Matoso, L.T. Kubota, S. Cadore, Use of silica gel chemically modified with zirconium phosphate for preconcentration and determination of lead and copper by flame atomic absorption spectrometry, *Talanta* 60 (2003) 1105–1111.
- [2] S. Tunali, A. Çabuk, T. Akar, Removal of lead and copper ions from aqueous solutions by bacterial strain isolated from soil, *Chem. Eng. J.* 115 (2006) 203–211.
- [3] Available from: <[http://www.who.int/water\\_sanitation\\_health/dwq/gdwq3rev/en/index.html](http://www.who.int/water_sanitation_health/dwq/gdwq3rev/en/index.html)>.
- [4] M. Kobya, E. Demirbas, E. Senturk, M. Ince, Adsorption of heavy metal ions from aqueous solutions by activated carbon prepared from apricot stone, *Bioreour. Technol.* 96 (2005) 1518–1521.
- [5] M. Hamidpour, M. Kalbasi, M. Afyuni, H. Shariatmadari, P.E. Holm, H.C. Hansen, Sorption hysteresis of Cd(II) and Pb(II) on natural zeolite and bentonite, *J. Hazard. Mater.* 181 (2010) 686–691.
- [6] K.G. Bhattacharyya, S.S. Gupta, Adsorptive accumulation of Cd(II), Co(II), Cu(II), Pb(II), and Ni(II) from water on montmorillonite: Influence of acid activation, *J. Colloid Interface Sci.* 310 (2007) 411–424.
- [7] K. Al-Zboon, M.S. Al-Harashsheh, F.B. Hani, Fly ash-based geopolymer for Pb removal from aqueous solution, *J. Hazard. Mater.* 188 (2011) 414–421.
- [8] M. Iqbal, A. Saeed, S.I. Zafar, FTIR spectrophotometry, kinetics and adsorption isotherms modeling, ion exchange, and EDX analysis for understanding the mechanism of  $\text{Cd}^{2+}$  and  $\text{Pb}^{2+}$  removal by mango peel waste, *J. Hazard. Mater.* 164 (2009) 161–171.
- [9] Z. Xuan, Y. Tang, X. Li, Y. Liu, F. Luo, Study on the equilibrium, kinetics and isotherm of biosorption of lead ions onto pretreated chemically modified orange peel, *Biochem. Eng. J.* 31 (2006) 160–164.
- [10] B.M.W.P.K. Amarasinghe, R.A. Williams, Tea waste as a low cost adsorbent for the removal of Cu and Pb from wastewater, *Chem. Eng. J.* 132 (2007) 299–309.
- [11] K.K. Wong, C.K. Lee, K.S. Low, M.J. Haron, Removal of Cu and Pb by tartaric acid modified rice husk from aqueous solutions, *Chemosphere* 50 (2003) 23–28.
- [12] T.K. Naiya, A.K. Bhattacharya, S.K. Das, Adsorption of Cd(II) and Pb(II) from aqueous solutions on activated alumina, *J. Colloid Interface Sci.* 333 (2009) 14–26.
- [13] R. Laus, T.G. Costa, B. Szpoganicz, V.T. Fávere, Adsorption and desorption of Cu(II), Cd(II) and Pb(II) ions using chitosan crosslinked with epichlorohydrin-triphosphate as the adsorbent, *J. Hazard. Mater.* 183 (2010) 233–241.
- [14] M.V. Dinu, E.S. Dragan, A.W. Trochimczuk, Sorption of Pb(II), Cd(II) and Zn(II) by iminodiacetate chelating resins in non-competitive and competitive conditions, *Desalination* 249 (2009) 374–379.
- [15] A. Demirbas, E. Pehlivan, F. Gode, T. Altun, G. Arslan, Adsorption of Cu(II), Zn(II), Ni(II), Pb(II), and Cd(II) from aqueous solution on Amberlite IR-120 synthetic resin, *J. Colloid Interface Sci.* 282 (2005) 20–25.
- [16] İ.A. Şengil, M. Özacar, Competitive biosorption of  $\text{Pb}^{2+}$ ,  $\text{Cu}^{2+}$  and  $\text{Zn}^{2+}$  ions from aqueous solutions onto valonia tannin resin, *J. Hazard. Mater.* 166 (2009) 1488–1494.
- [17] A.H. Hawari, C.N. Mulligan, Biosorption of lead(II), cadmium(II), copper(II) and nickel(II) by anaerobic granular biomass, *Bioreour. Technol.* 97 (2006) 692–700.
- [18] A.Y. Dursun, A comparative study on determination of the equilibrium, kinetic and thermodynamic parameters of biosorption of copper(II) and lead(II) ions onto pretreated *Aspergillus niger*, *Biochem. Eng. J.* 28 (2006) 187–195.
- [19] A. Singh, D. Kumar, J.P. Gaur, Copper(II) and lead(II) sorption from aqueous solution by non-living *Spirogyra neglecta*, *Bioreour. Technol.* 98 (2007) 3622–3629.
- [20] P. Pavasant, R. Apiratikul, V. Sungkhum, P. Suthiparinyanont, S. Wattanachira, T.F. Marhaba, Biosorption of  $\text{Cu}^{2+}$ ,  $\text{Cd}^{2+}$ ,  $\text{Pb}^{2+}$ , and  $\text{Zn}^{2+}$  using dried marine green macroalga *Caulerpa lentillifera*, *Bioreour. Technol.* 97 (2006) 2321–2329.
- [21] X. Bai, Z. Ye, Y. Li, L. Yang, Y. Qu, X. Yang, Preparation and characterization of a novel macroporous immobilized micro-organism carrier, *Biochem. Eng. J.* 49 (2010) 264–270.
- [22] Q. Liao, J. Sun, L. Gao, The adsorption of resorcinol from water using multi-walled carbon nanotubes, *Colloids Surf. A: Physicochem. Eng. Aspects* 312 (2008) 160–165.
- [23] M. Abdel Salam, M. Mokhtar, S.N. Basahel, S.A. Al-Thabaiti, A.Y. Obaid, Removal of chlorophenol from aqueous solutions by multi-walled carbon nanotubes: Kinetic and thermodynamic studies, *J. Alloys Compd.* 500 (2010) 87–92.
- [24] G.C. Chen, X.Q. Shan, Y.Q. Zhou, X.E. Shen, H.L. Huang, S.U. Khan, Adsorption kinetics, isotherms and thermodynamics of atrazine on surface oxidized multiwalled carbon nanotubes, *J. Hazard. Mater.* 169 (2009) 912–918.
- [25] C. Lu, F. Su, S. Hu, Surface modification of carbon nanotubes for enhancing BTEX adsorption from aqueous solutions, *Appl. Surf. Sci.* 254 (2008) 7035–7041.

- [26] Y. Yao, F. Xu, M. Chen, Z. Xu, Z. Zhu, Adsorption behavior of methylene blue on carbon nanotubes, *Bioresour. Technol.* 101 (2010) 3040–3046.
- [27] C.H. Wu, Adsorption of reactive dye onto carbon nanotubes: Equilibrium, kinetics and thermodynamics, *J. Hazard. Mater.* 144 (2007) 93–100.
- [28] Y.H. Li, J. Ding, Z. Luan, Z. Di, Y. Zhu, C. Xu, D. Wu, B. Wei, Competitive adsorption of  $Pb^{2+}$ ,  $Cu^{2+}$  and  $Cd^{2+}$  ions from aqueous solutions by multiwalled carbon nanotubes, *Carbon* 41 (2003) 2787–2792.
- [29] M.A. Tofiqhy, T. Mohammadi, Adsorption of divalent heavy metal ions from water using carbon nanotube sheets, *J. Hazard. Mater.* 185 (2011) 140–147.
- [30] C. Chen, J. Hu, D. Shao, J. Li, X. Wang, Adsorption behavior of multiwall carbon nanotube/iron oxide magnetic composites for Ni(II) and Sr(II), *J. Hazard. Mater.* 164 (2009) 923–928.
- [31] A. Idris, N.A.M. Zain, M.S. Suhaimi, Immobilization of Baker's yeast invertase in PVA–alginate matrix using innovative immobilization technique, *Process Biochem.* 43 (2008) 331–338.
- [32] X. Ren, C. Chen, M. Nagatsu, X. Wang, Carbon nanotubes as adsorbents in environmental pollution management: A review, *Chem. Eng. J.* 170 (2011) 395–410.
- [33] R.K. Xu, Y. Wang, D. Tiwari, H.Y. Wang, Effect of ionic strength on adsorption of As(III) and As(V) on variable charge soils, *J. Environ. Sci.* 21 (2009) 927–932.
- [34] E. Repo, J.K. Warchol, T.A. Kurniawan, M.E.T. Sillanpää, Adsorption of Co(II) and Ni(II) by EDTA- and/or DTPA-modified chitosan: Kinetic and equilibrium modeling, *Chem. Eng. J.* 161 (2010) 73–82.
- [35] M. Jain, V.K. Garg, K. Kadirvelu, Chromium(VI) removal from aqueous system using *Helianthus annuus* (sunflower) stem waste, *J. Hazard. Mater.* 162 (2009) 365–372.
- [36] X.J. Hu, J.S. Wang, Y.G. Liu, X. Li, G.M. Zeng, Z.L. Bao, X.X. Zeng, A.W. Chen, F. Long, Adsorption of chromium (VI) by ethylenediamine-modified cross-linked magnetic chitosan resin: Isotherms, kinetics and thermodynamics, *J. Hazard. Mater.* 185 (2011) 306–314.
- [37] A. Sari, M. Tuzen, Kinetic and equilibrium studies of biosorption of Pb(II) and Cd(II) from aqueous solution by macrofungus (*Amanita rubescens*) biomass, *J. Hazard. Mater.* 164(2–3) (2009) 1004–1011.
- [38] R.A. Anayurt, A. Sari, M. Tuzen, Equilibrium, thermodynamic and kinetic studies on biosorption of Pb(II) and Cd(II) from aqueous solution by macrofungus (*Lactarius scrobiculatus*) biomass, *Chem. Eng. J.* 151 (1–3) (2009) 255–261.
- [39] K. Srividya, K. Mohanty, Biosorption of hexavalent chromium from aqueous solutions by *Catla catla* scales: Equilibrium and kinetics studies, *Chem. Eng. J.* 155(3) (2009) 666–673.
- [40] W.J. Weber, J.C. Morris, Kinetics of adsorption on carbon solution, *J. Sanit. Eng. Div. ASCE* 89 (1963) 31–60.
- [41] E. Erdem, N. Karapinar, R. Donat, The removal of heavy metal cations by natural zeolites, *J. Colloid Interface Sci.* 280 (2004) 309–314.
- [42] P.C. Mishra, R.K. Patel, Removal of lead and zinc ions from water by low cost adsorbents, *J. Hazard. Mater.* 168 (2009) 319–325.
- [43] D. Feng, J.S.J. van Deventer, C. Aldrich, Removal of pollutants from acid mine wastewater using metallurgical by-product slags, *Sep. Purif. Technol.* 40 (2004) 61–67.
- [44] N. Ünlü, M. Ersoz, Removal of heavy metal ions by using dithiocarbamated- sporopollenin, *Sep. Purif. Technol.* 52 (2007) 461–469.
- [45] S.G. Wang, W.X. Gong, X.W. Liu, Y.W. Yao, B.Y. Gao, Q.Y. Yue, Removal of lead(II) from aqueous solution by adsorption onto manganese oxide-coated carbon nanotubes, *Sep. Purif. Technol.* 58 (2007) 17–23.
- [46] Y. Li, F. Liu, B. Xia, Q. Du, P. Zhang, D. Wang, Z. Wang, Y. Xia, Removal of copper from aqueous solution by carbon nanotube/calcium alginate composites, *J. Hazard. Mater.* 177 (2010) 876–880.
- [47] S. Patachia, R. Dobritoiu, T. Coviello, Determination of the sorption efficiency of poly (vinyl alcohol)/ Scleroglucan cryogels, against  $Cu^{2+}$  ions, *Environ. Eng. Manage. J.* 10 (2011) 193–198.